

# The Effect of Forming Temperature on the Microstructure and Stress Distribution for Lead Babbitt Alloy in Hot Backward Extrusion Process

Prof. Dr. Adnan Naama Abood    Asst. prof. Dr. Ali Hasan Saleh    Muntadher AbdulZahra Hasan\*  
Technical Engineering College-Baghdad, Middle Technical University  
\*E-mail: muntadhero@yahoo.com

## Abstract

This study aims to modify the microstructure and mechanical properties of Babbitt alloy (ASTM B23 alloy 13). Two casting techniques were implemented to manufacture the alloy; Gravity Die Casting (GDC) and New Rheocasting (NRC) techniques. The microscope examination shows that the structures contained two phases,  $\alpha$ -Pb and cubic shaped intermetallic compound ( $\beta$ -SbSn) in a matrix of ternary phases. GDC structure was a dendrite  $\alpha$ -Pb phase, while the equiaxed structure was observed via NRC, with remaining  $\beta$ -SbSn phase as a cubic shape. The manufactured Babbitt alloy by NRC has the best compression and yield strength, while the castings produced by GDC recorded lower properties. Backward extrusion was used to improve the properties of alloy 13 produced by two casting techniques. The backward extrusion were carried in the temperature range of 20-100°C. NRC samples showed the highest mechanical properties under all extruded conditions. The enhanced mechanical properties were mainly attributed to the grain refinement. FEM-simulation code DEFORM 3D was used to investigate the stress distribution in backward extrusion process of billet. Highest effective stress exists in the transition area between bottom and wall of the workpiece (punch corner). At the inner side of the wall, stress is higher than at the outer side of wall.

**Keywords:** lead Babbitt alloy, gravity die casting, new rheocasting, backward extrusion, microstructure, mechanical properties, FEM-simulation.

## 1. Introduction

Babbitt alloys (white metals) since to the patent 1252 was granted to Isaac Babbitt in 1839. The patent describes the use of tin-base white metal bearings backed by stronger shell line- bearing box in the 1930. The metal was refined to be optimized for bearing applications. The term Babbitt alloys is used today for tin-as well as lead-based alloys [1]. Lead-based white metals exhibit a lower friction coefficient, better, bonding to the shells, and better properties for casting and extrusion than tin-based alloys. However, the increase in use of lead-based white metal is attributed mostly to its lower cost. These alloys are generally alloyed with 10-15wt% antimony and 0.5-8wt% tin. Antimony (Sb) strengthens the matrix by solid solution hardening and with Tin (Sn) forms the  $\beta$ -phase (SnSb). This intermetallic compound is found as small cuboids dispersed in the matrix, but they do not have a significant adverse effect on the frictional properties because the soft matrix spreads out on the surface during sliding to form a thin lubricating film [2]. This may be achieved through microstructural grain refinement. The grain refinement is believed as the most effective mechanism to accomplish both the desired strength and ductility at ambient temperature [3]. The microstructure properties of Lead-based alloy can be controlled by different methods such as the casting techniques and backward extrusion [4, 5]. By using different casting techniques, hundreds of bearing materials have been developed in the recent time which offers promising individual properties to meet particular service requirements. There are two common casting techniques. One is gravity die casting, a technique of fully dendritic microstructure. The other is new rheocasting, which involves the application of shearing during solid fixation to produce a non-dendritic semi-solid slurry which is transferred directly into a mould or die to produce a final product [6]. In order to obtain much more enhanced mechanical properties and wear resistance, accordingly, a proper control of the manufacturing conditions and best understanding of the relations between the microstructure and mechanical properties of backward extruded lead alloy have become one of the most important on-going research areas [7, 8]. The backward extrusion method has been successfully utilized as a final processing method to produce fine grained products. Consequently this route has become one of the most effective manufacturing processes due to its proper stress distributions, material savings, and lower required machining [9, 10].

## 2. Experimental Procedures

### 2.1 Material Billet Preparation

The material used for backward extrusion was lead Babbitt (ASTM B23 Alloy 13) produced by two casting techniques Gravity Die Casting (GDC) and New Rheocasting (NRC). Gravity die castings were manufactured in mould made of AISI H13 steel mould of 60x60x120mm with thickness of 20mm. Two K-type thermocouples with 3mm in diameter covered with stainless steel sheath were employed. The first thermocouple was used to

measure the pouring temperature and other was fixed in the mould wall through hole to ensure positive contact between the sensor tip of thermocouple and the molten to determine cooling rate during solidification. The molten metal was poured at a temperature of 370°C then left to solidify at room temperature of the inclined mould [11].

New Rheocasting were produced in mould made of AISI 304 austenitic stainless steel of 60x60x120mm. For increasing the contact area among molten metal and die wall, the die is inclined at an angle of 75° to give a good occasion for crystals forming on the wall and increase the distance of metal flow which helps in increasing the probability of separating the freezing crystals from the die wall [12]. Thermocouple and the procedure used in previous methods were also used in this casting technique. The molten metal at temperature of 265°C was poured on the wall of the inclined mould. When temperature reached approximately 230°C (this temperature at liquid -solid interface) the mould was water cooled (quenched). The billets are cylindrical specimens with 24 mm in diameter and 30 mm height, cut and machined from the casting (60x60x120mm) for GDC and NRC techniques.

## 2.2 Backward Extrusion

Figure (1) shows the schematic diagram of the die of backward extrusion. The extrusion process was performed using a hydraulic press (maximum force: 1400 KN, maximum stroke: 500 mm). The billet is reheated at forming temperature using induction system. Billet was positioned in the center of the inductor

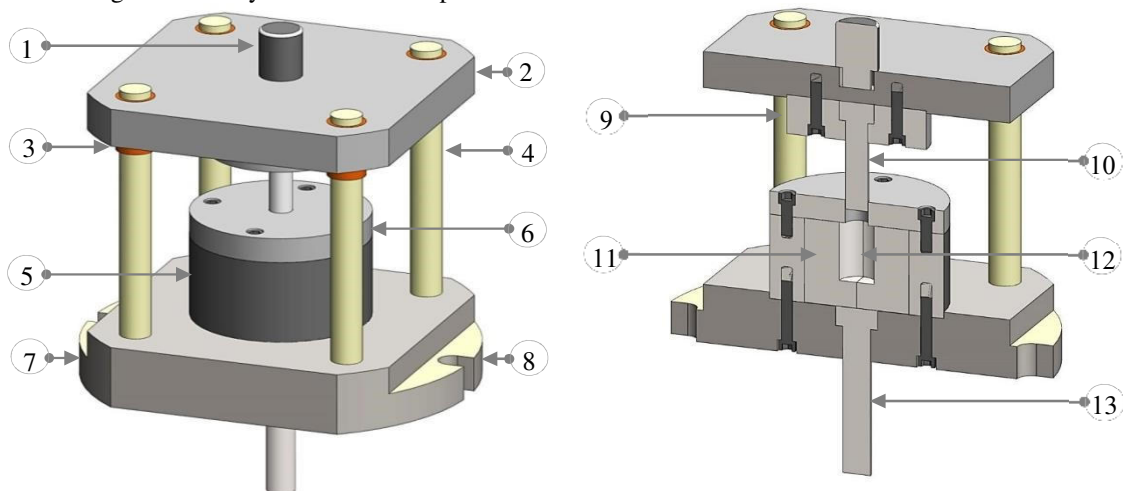


Figure (1); Schematic diagram of die of backward extrusion: 1 -Shank; 2- Upper Plate; 3-Bush; 4-Guide; 5- Supporter Ring; 6- Stripper; 7- Lower Plate; 8-Fix; 9- Punch Holder; 10-Punch; 11-Die; 12-Billet; 13-Ejector coil. This heating system is controlled by an electronic device which programs the reheating cycles see Figure (2). Two “K” type thermocouples were inserted to monitor the temperature evolution: the first one into the center of the billet and the second one was into the die at less than 5 mm from the billet surface.

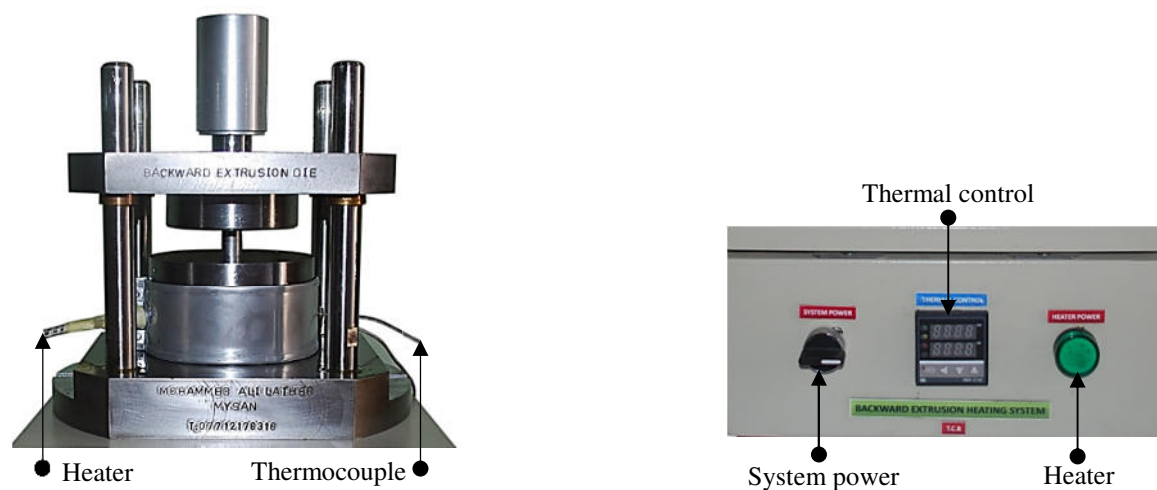


Figure (2); Heating system

### 2.3 Foundation of Simulation Model

In this work, the effect of forming temperature on stress distribution during backward extrusion process was investigated by numerical simulation (using DEFORM.3D V10.2). Figure (3) shows the geometric the geometric model in this simulation, and a half is adopted for its symmetrical character. In this simulation, ASTM B23 Alloy 13 was defined as an isotropic hardened. The constitutive equation in this simulation is as follows [13]:

$$\bar{\sigma} = \sigma(\epsilon, \dot{\epsilon}, T)$$

$\bar{\sigma}$  is the mean stress,  $\sigma$  is the yield stress,  $\epsilon$  is the equivalent strain  $\dot{\epsilon}$  is the strain rate and T is the temperature. The true stress–true strain response of alloy 13 compressed at 20 and 100°C under the strain rate of  $10^{-3}/\text{sec}^{-1}$  for gravity die casting and new rheocasting techniques. Were inputted into material storage, and the flow stress model was established by using log-log space linear differential analysis.

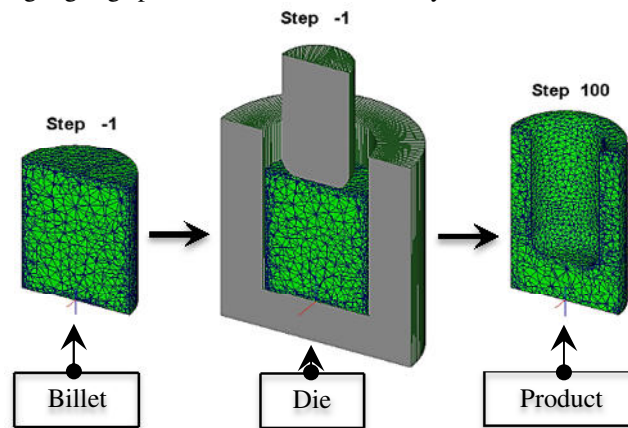


Figure (3); Geometric model

### 2.4 Microstructure Characterization

In general, the microstructure of lead Babbitt Alloy 13 consists of two phases, the Dark phase  $\alpha$ -Pb and the white cubic phase  $\beta$ -SbSn in a soft matrix of ternary eutectic formed from the dark phase  $\alpha$ -Pb, white cubic phase  $\beta$ -SbSn and Sb-rich solid solution was also white. The extruded samples cutting to vertically section (Figure 4). Four regions of the wall samples were chosen to be investigated, at 1, 2, 3, and 4mm from the inner edge. Because the microstructure of wall similar to bottom when extrude with contact ratio 0.5 (contact ratio is punch flatness divided on punch diameter) [14].

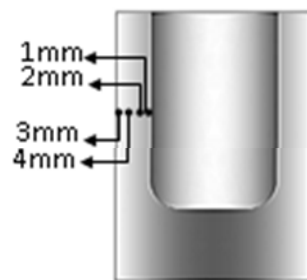


Figure (4); The specimen of microstructure

### 2.5 Mechanical Properties

The microhardness test was carried out using Vickers hardness tester. The test load and dwelling time were 100g and 15s respectively according to ASTM-E384. Microhardness measurement selected at four positions from the inner to the outer edge. To approach the actual assessment, extruded samples and casting were selected for compression test with a certain dimension specimens with the dimension of diameter and the height of compression samples were 25 mm and 30 mm, respectively.

### 2.6 XRD Analysis

The samples with the dimension of 14mm in diameter and 5mm in height used for x-ray diffraction analysis. This analysis method was performed to investigate alloy phases formed during two casting techniques. X-ray type: Philips pw/840 Holland, Cu target, Ni filter, scan speed 3 degree/min, voltage: 40 K.V and current: 20 mille ampere, was used for detecting the phases as shown in Figure (5).

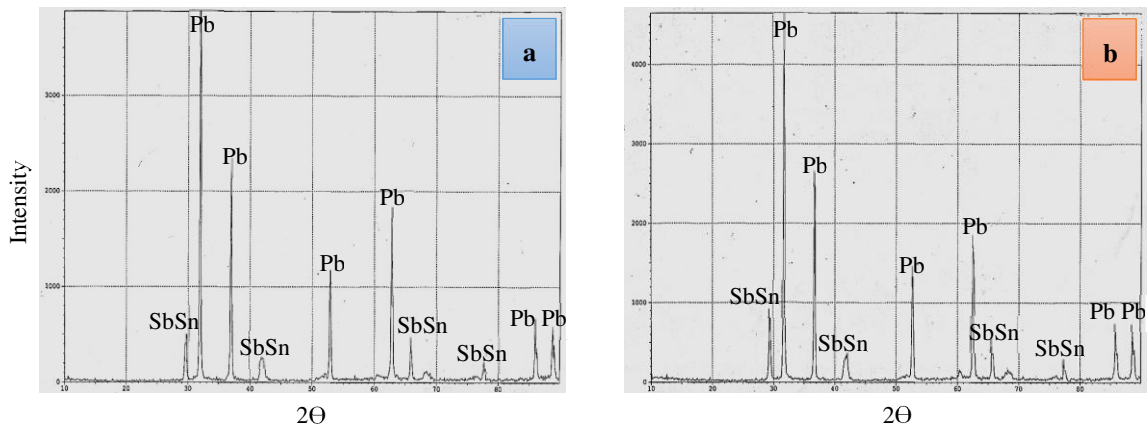


Figure (5); X-Ray diffraction analysis a: DC and b: NRC

### 3. Results and discussion

#### 3.1 Microstructure of Casting

The microstructure obtained from GDC was dendritic  $\alpha$ -Pb primary phase formed from the wall to the center with different DAS sizes are shown in Figure (6). The measurement of average DAS indicates that variation from the wall to center, at distance of 2, 7, 15 and 30mm, where they are 15, and 26, 27 and 34  $\mu\text{m}$  respectively. This increasing in DAS toward the center is due to the decrease in cooling rate with increasing the distance from the wall [15]. Coarsening in a cubic  $\beta$ -SbSn phase was observed in coarse soft matrix ternary eutectic with an average size of 13, 18, 23 and 31  $\mu\text{m}$ , at 2,7,15 and 30 mm respectively.

The microstructure examination of new rheocasting showed fine cluster equiaxed grain from  $\alpha$ -Pb phase rather than dendritic structure with difference grain size (Figure 7). The average grain size at the 2mm is roughly 13 $\mu\text{m}$  due to high thermal gradient in water cooling. Moreover, a low volume fraction of  $\beta$ -SbSn with average size equal 12 $\mu\text{m}$  was observed in fine eutectic. At 7mm from the wall it was recognized of 19 $\mu\text{m}$  and 14 $\mu\text{m}$  grain size of  $\beta$ -SbSn. Average grain size of  $\alpha$ -Pb and  $\beta$ -SbSn phase with the eutectic coarseness increase at distance of 15mm from the wall. Sizes of  $\alpha$  and  $\beta$  are 21 $\mu\text{m}$  and 16 $\mu\text{m}$  respectively. Coarser equiaxed grain of  $\alpha$ -phase with reduction in volume fraction is showed at the 30mm center of casting with the size of 25 $\mu\text{m}$ . while a cubic phase (SbSn) with average size equal to 22 $\mu\text{m}$ . Furthermore, the cubic  $\beta$ -SbSn phase is finer than gravity die casting, from the wall to center of casting.

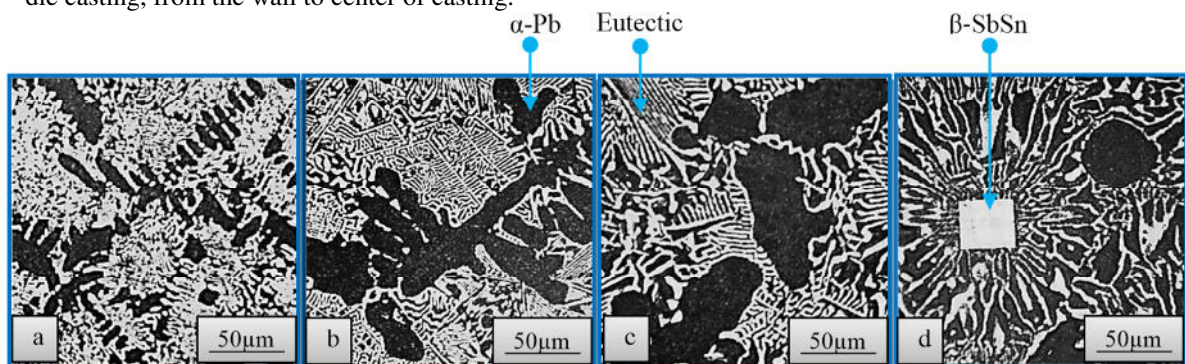


Figure (6); GDC Microstructure

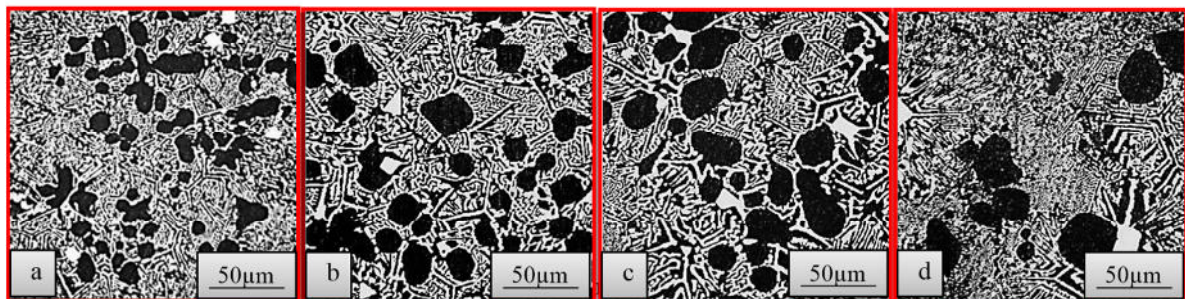


Figure (7); NRC Microstructure

a: at 2mm, b: at 7mm, c: at 15mm and d: at 30mm

### 3.2 Forming Force

The force required for backward extrusion decreases with increasing billet temperature for the all samples extruded at constant area reduction and contact ratio are present in Figure (8). It is clear that the maximum force of 83.9 and 89KN for GDC and NRC, respectively at room temperature. While at temperature 100°C the force recorded 36 and 38.2KN for GDC and NRC. The matter is attributed to the maximum plastic strain that is occurred with increasing temperature and that conform to results of S. Enayati et al [16].

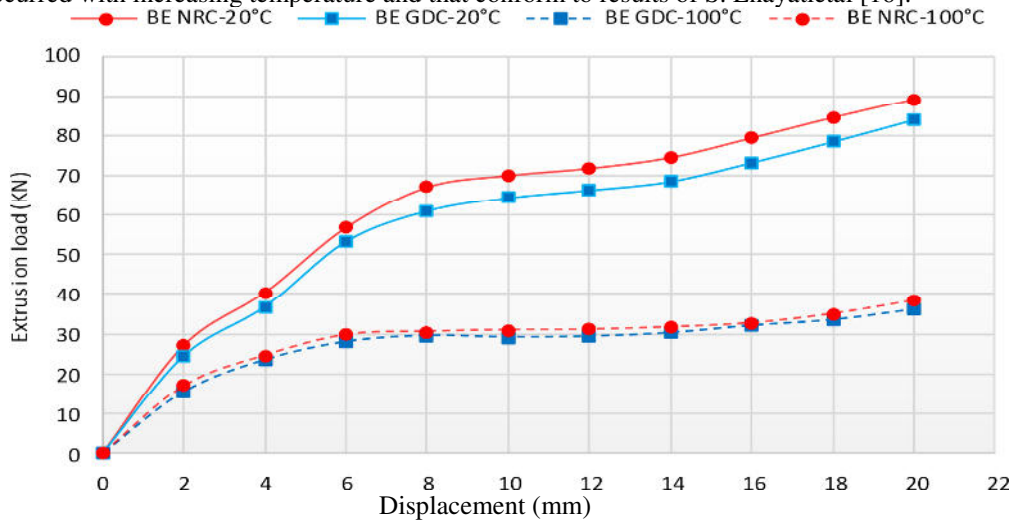


Figure (8); Effect of temperature on force required for backward extrusion

### 3.3 Backward Extruded Microstructure

The extruded microstructure of both conventional gravity die cast and new rheocast show that phases are uniformly distributed. It contained four distinct regions marked at 1, 2, 3, and 4mm, from center to surface (Figure 4). The primary  $\alpha$ -Pb and  $\beta$ -SbSn phase in both cases was very small at the specimen center, and gradually increases toward to the surface region. In the surface the grain size was bigger and thicker. It is also observed that at center, the primary  $\alpha$ -Pb is elongated in direction of extrusion and the  $\beta$ -SbSn phase fragmented to small parts. The material at this region underwent severe plastic deformation, and the fine grains indicate that recrystallization has occurred. These microstructure changes during the backward extrusion process were closely related to forming temperature varying at different positions [17].

Figure (9) shows the microstructures at room temperature of both GDC and NRC samples. The grain size of  $\alpha$ -Pb and  $\beta$ -SbSn phase for GDC was 13-25 $\mu$ m, and  $\beta$ -SbSn phase 11-16 $\mu$ m, respectively. Whereas grain size of NRC was 8-13 $\mu$ m of  $\alpha$ -Pb and 7-11 $\mu$ m of  $\beta$ -SbSn phase are presented in (10). Compared with microstructure at 100°C as shown in Figure (11), it was noticed that grain size of  $\alpha$ -Pb for GDC was 13-25 $\mu$ m, and  $\beta$ -SbSn phase 11-16 $\mu$ m. While,  $\alpha$ -Pb and  $\beta$ -SbSn grain size of NRC were 8-13  $\mu$ m and 7-11  $\mu$ m, respectively (Figure 12).

The forming temperature plays an important role in the formation of finer microstructures. In fact decreasing the forming temperature lead to finer microstructure. This explained the fact that as the temperature increases, the size of dynamically recrystallized grain increases [18].

### 3.4 Vickers Microhardness

The effect of forming temperature on the hardness of Back Extrusion (BE) GDC and BE NRC samples at four positions was recorded from the inner to the outer edge (Figure 13). The hardness is improved with the decreasing forming temperature. This phenomenon was also observed in other metal [18]. Hardness of the BE NRC, is higher than of BE GDC at all temperature. The reason is attributed to the grain size in NRC was smaller than that of GDC [19]. The results show also the inner edge have the maximum hardness and the hardness decreased gradually from the inner toward the outer edge of the extruded part. Because an inner edge, which was directly compressed. The grain size in this region was finer than that of outer edge.

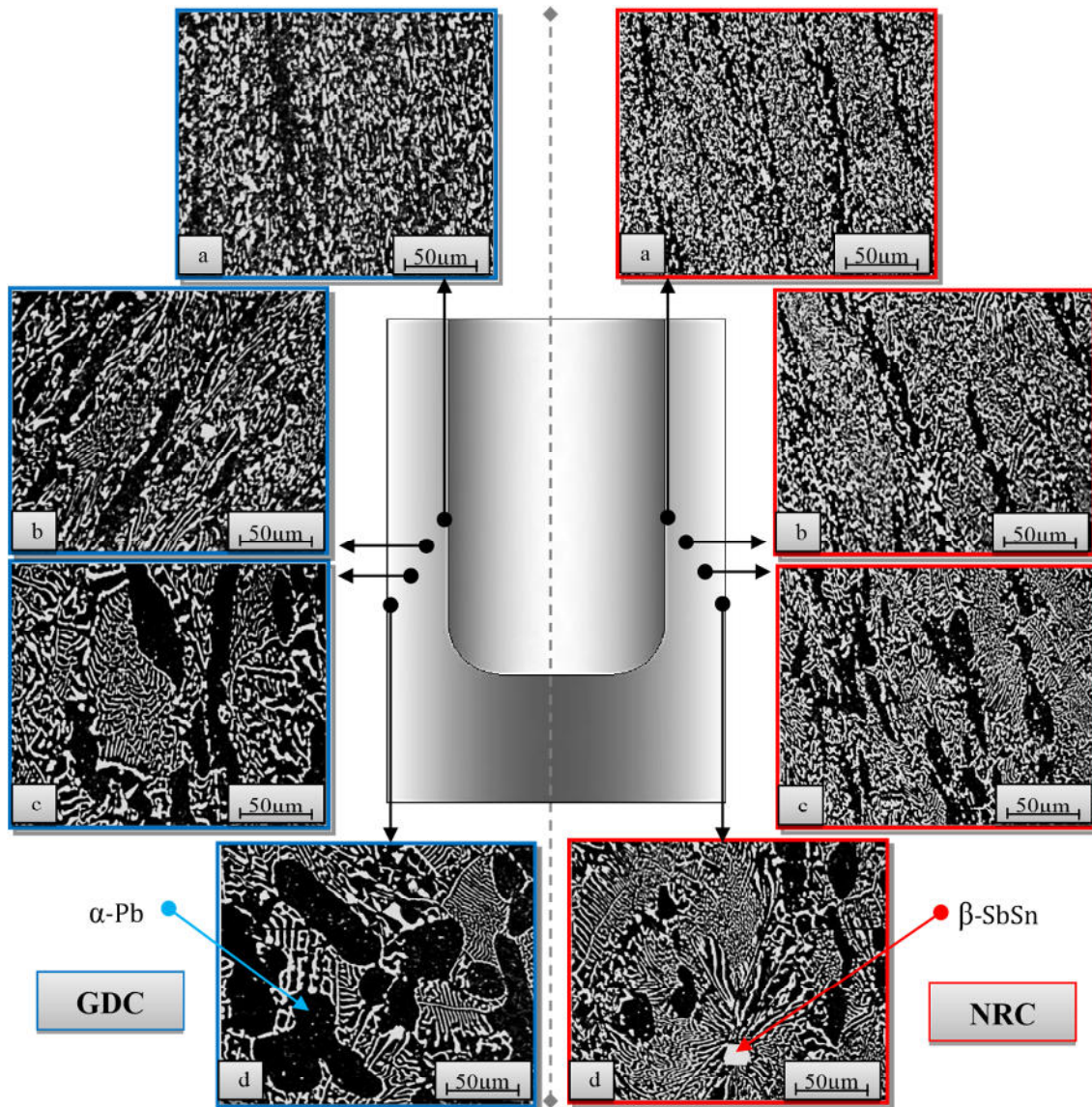


Figure (9); The Microstructure of BE GDC and BE NRC at 20°C with 40% r and 0.5 Rc  
 a: at 1mm, b: at 2mm, c: at 3mm, and d: at 4mm

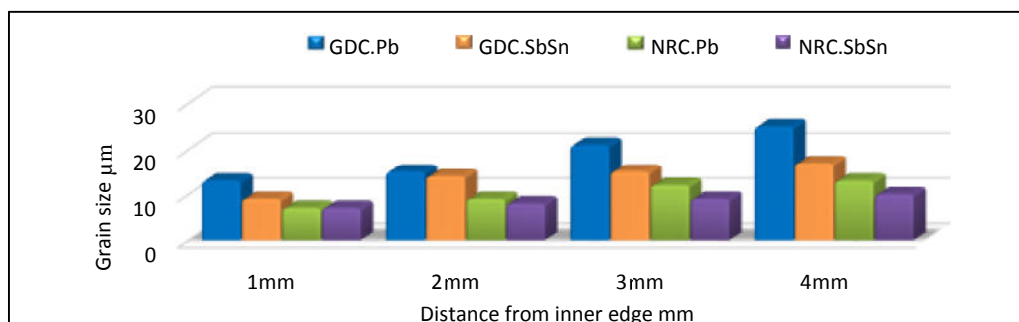


Figure (10); Grain size at 20°C

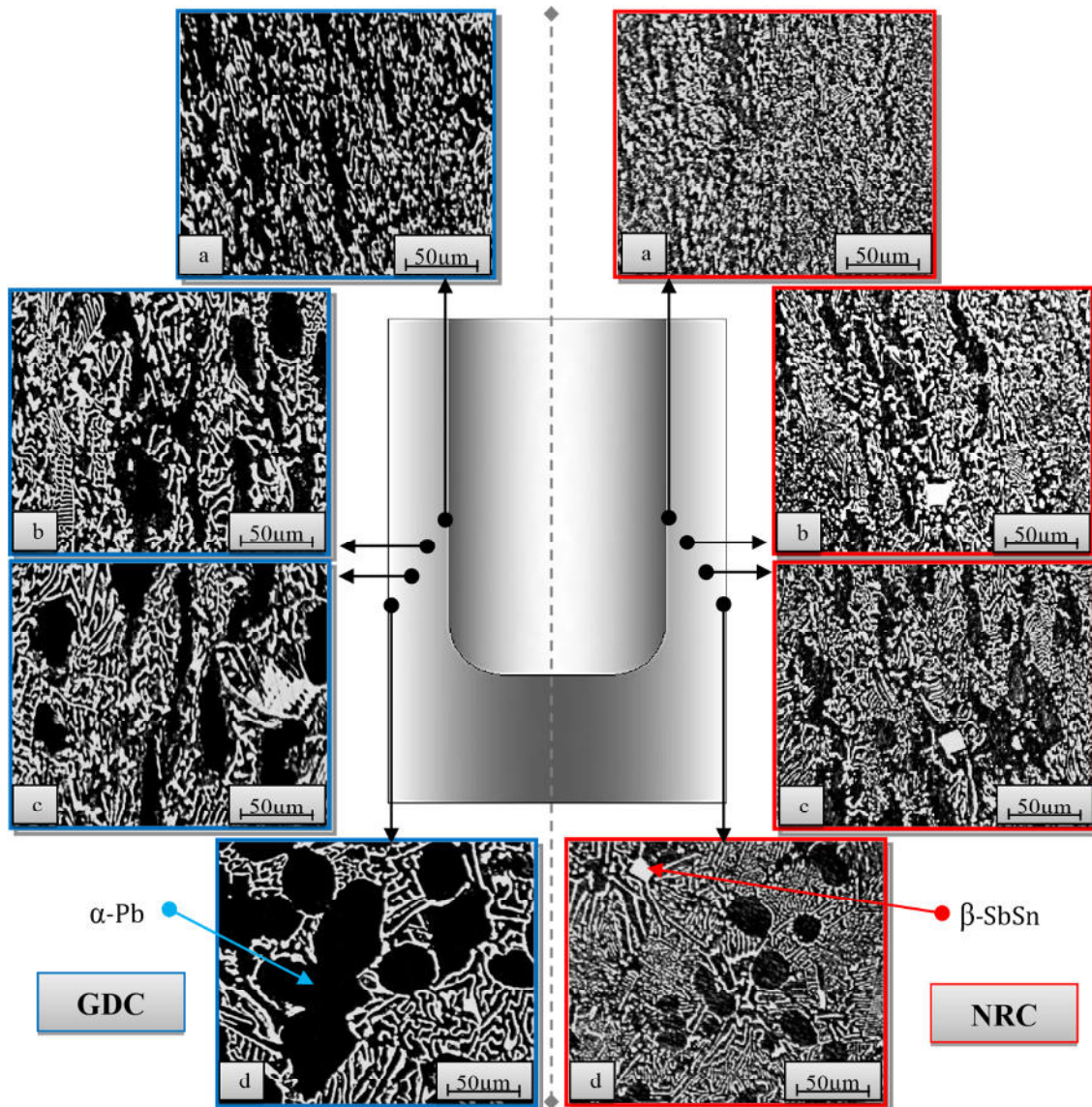


Figure (11); The Microstructure of BE GDC and BE NRC at 100°C with 40% r and 0.5 Rc  
 a: at 1mm, b: at 2mm, c: at 3mm, and d: at 4mm

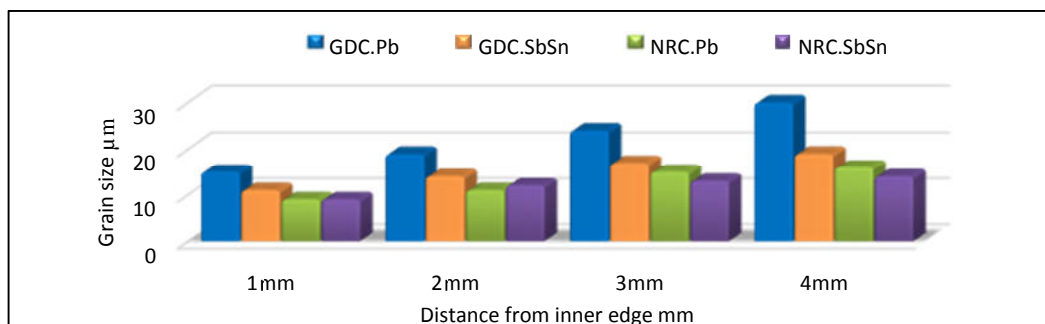


Figure (12); Grain size at 100°C

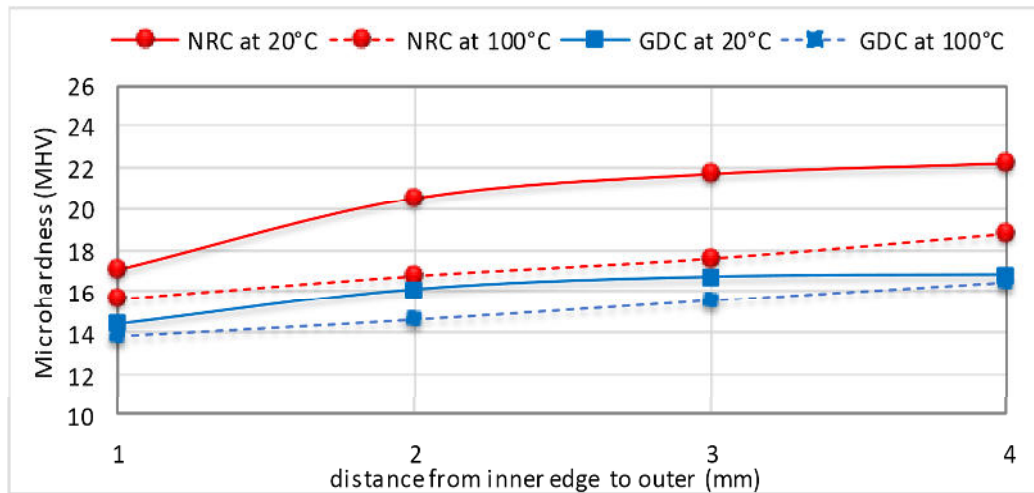


Figure (13); Microhardness measurement

### 3.5 Mechanical Properties

At room temperature, the yield strength, compression strength and elongation are improved by backward extrusion process as shown in Table (1). The BENRC alloy exhibits the optimal mechanical properties. Whereas, the values of compressive yield strength and compressive strength were 68MPa and 80MPa, respectively. The high mechanical properties are mainly attributed to formation of fine grain microstructures. Accordingly, it is expected that the dislocation movement is restricted, when the grain size is decreased, thereby higher stress is needed for further deformation. While, the elongation of BEGDC samples have maximum value of 6.2%. Furthermore, the mechanical properties of the NRC were better than the GDC at different condition.

Table (1); Mechanical properties of alloy 13

Material	Property	Compression strength MPa	Yield strength MPa	Elongation%
GDC		59	42	2.7
NRC		66	54	2.3
BE GDC		73	51	6.2
BE NRC		80	68	5.1

### 3.6 Surface Roughness

The surface roughness is increasing with increasing forming temperature. The average surface roughness (Ra) of the GDC is 0.19 $\mu$ m which is significant as compared to the NRC at room temperature 0.15 $\mu$ m (Table 2). The surface roughness in the samples is the function of forming temperature and mechanical properties of the alloy. Balusamy et al [20] have reported that the surface roughness and its distribution in the samples depend on mechanical properties of the alloy.

Table (2); Roughness of extruded alloy 13

Material	Temperature	Roughness (Ra $\mu$ m)
GDC	20°C	0.19
NRC	20°C	0.15
GDC	100°C	0.57
NRC	100°C	0.16

### 3.7 Effective Stress distribution

Effective Stress distribution for GDC and NRC at room temperature, are represented by Figure (14). The lowest values of effective stress occur at the wall head of the specimen where material flow hardly takes place. In the workpiece region directly below the punch head there is also restricted material flow. Absolute highest effective stress exists in the transition area between bottom and wall of the workpiece (punch corner). At the inner side of the wall stress are higher than outer side of the wall. The effective stress was still largest for the last step. With increasing forming temperature (Figure 15), the effective stress reduces whereas at 100°C they have the largest decrease. But no significant difference in the stress distribution for gravity die casting and new rheocasting samples in backward extrusion at constant temperature.

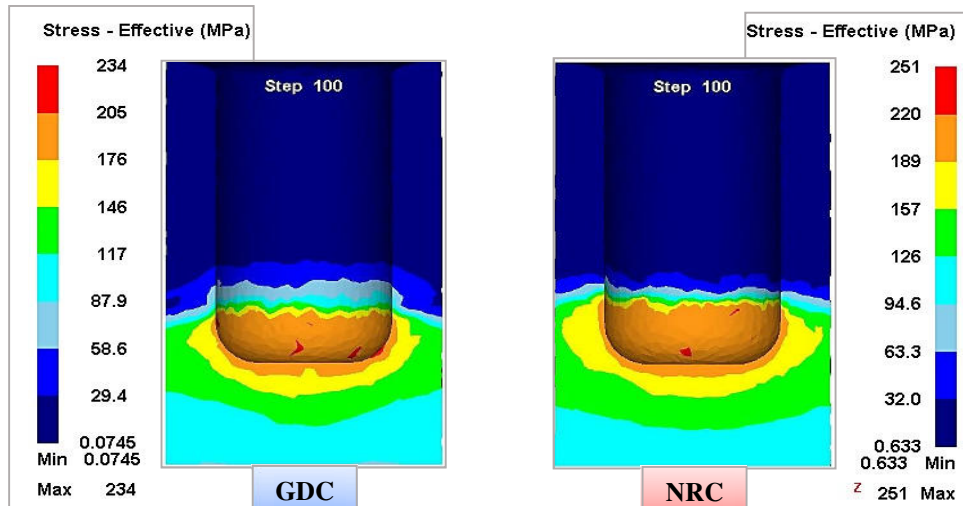


Figure (14); Effective stress distribution at 20°C

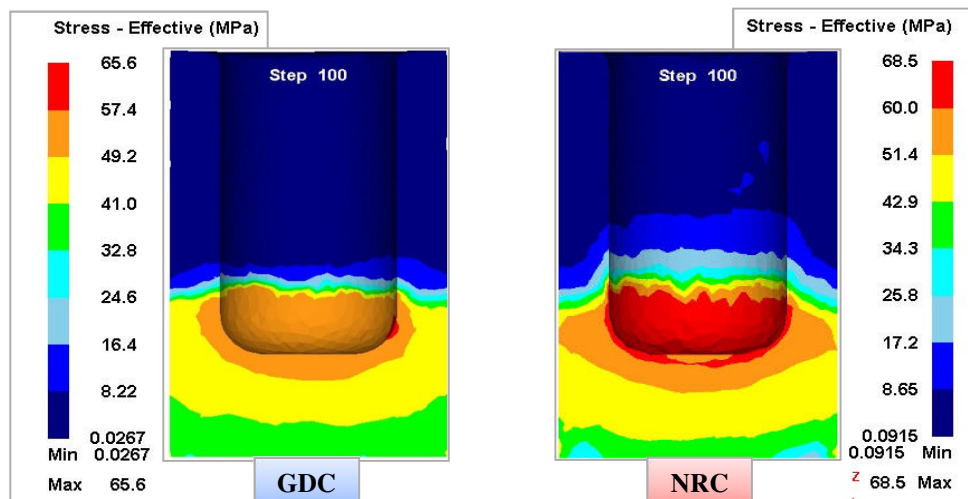


Figure (15); Effective stress distribution at 100°C

#### 4. Conclusions

- With decreasing Forming temperature of extruded products, the grain size is refined and Normal applied load will be increased.
- Increasing Forming temperature has negative effect on compression, yield strength, hardness and roughness, while increase the elongation.
- The New Rheocasting products had recorded the maximum compression and yield strength as well as the hardness, whereas the gravity die casting had recorded the minimum.
- The highest values of effective stress exist in the region around the punch corner whereas the lowest values of stress occur at the bottom of the specimen.

#### References

- [1] T. Teker and M. Kaplan, "The Effect of Co and Cr Particles Additions on Microstructure and Wear Behavior of Pb-Sn Based Alloy", Journal of Alloys and compounds, Vol.484, No.1, 2009, pp 510-513.
- [2] R. Schouwenaars, J. I. Romero, V. H. Jacobo, A. Ortiz, "Microstructures of Rapidly Solidified Pb-Sb-Sn alloys", Advanced Materials Research, Vol.15, No.17, 2007, pp 621-626.
- [3] P. Sriram and Ch. Visweswara, "Recent Developments in Cast Non-Ferrous Bearing Materials", Metal World, Vol.1, No.1, 2006, pp 6-10.
- [4] C. I. Nwoye and S. I. Okeke, "Improvement of the Mechanical Properties of Pb-Sb Alloy System through its Microstructural Modification by Copper Powder Dispersion during Casting", New York Science Journal, Vol.2, No.6, 2009, pp 86-92.
- [5] S. Eckert, B. Willers, P. A. Nikrityuk, K. Eckert, U. Michel and G. Zouhar, "Application of a Rotating

Magnetic Field during Directional Solidification of Pb-Sn Alloys ", *Materials Science and Engineering* Vol.413, No.414, 2005, pp 211-216.

- [6] B.Rahimi, M. Haddad-Sabzevar, "Effect of Rheocasting and Heat Treatment on Microstructure Characteristics and Mechanical Properties of High Performance 2024 Aluminum Alloy " Department of Metallurgy and Materials Engineering, Faculty of Engineering, The second International and the Seventh Joint Conference of Iranian Metallurgical Engineering and Iranian Foundryman Scientific Societies ,Ferdowsi University of Mashhad, Azadi Square, P.O. Box 91775, 1111, Mashhad, Iran.
- [7] S. A. Sadough, M.R. Rahmani, V. Pouyafar," Rheological behavior, Microstructure and Hardness of A356 Aluminum Alloy in Semisolid State Using Backward Extrusion Process " *Trans. Nonferrous Met. Soc. China* Vol. 20, 2010, pp 906–910.
- [8] E.R. de Freitas Jr., E. Ferracini, M. Ferrante, "Microstructure and Rheology of an AA2024 Aluminium Alloy in The Semi-Solid State, and Mechanical Properties of a Back-Extruded Part" *Mater. Process. Technol.* Vol.146, 2004, pp 241–249.
- [9] D. Hinza, A. Kirchnera, D.N. Brownb, B.M. Mab, O. Gutfleischa," Near Net Shape Production of Radially Oriented NdFeB Ring Magnets by Backward Extrusion " *Mater. Process. Technol.* Vol.135, 2003, pp 358–365.
- [10] T. Sheppard, P.J. Tunnicliffe, S.J. Patterso," Direct and Indirect Extrusion of a High Strength Aerospace Alloy (AA 7075)" *Mech. Work Technol.* Vol.6, 1982, pp 313–331.
- [11] Madhusudan, Narendranaath, Mohankmar, Mukunda, "Effect of Mould Wall Thickness on Rate of Solidification of Centrifugal Casting", *International Journal of Engineering Science and Technology*, Vol.2, No.11, 2010, pp 6092-6096.
- [12] A.N. Abood, "Design and Characterization of Advanced Semi-Solid Casting Processes", Ph. D. Thesis Submitted to the Department of Production Engineering and Metallurgy University of Technology, 2003.
- [13] Karen Abrinia, and Sakineh Orangi," Numerical Study of Backward Extrusion Process Using Finite Element Method", University of Tehran, School of Mechanical Engineering, College of Engineering, 2010, pp 381-405.
- [14] Ban Bakir Alamer, "The Study of Stress State in Indentation of a Flat Punch with Rounded Edge in Axisymmetric Backward Extrusion", *International Journal of Mining, Metallurgy & Mechanical Engineering (IJMMME)*, Vol. 1, Issue 2 ,2013, pp 2320–4060.
- [15] Palash Poddar n and K.L.Sahoo," Microstructure and Mechanical Properties of Conventional Cast and Rheocast Mg–Sn Based Alloys", *Materials Science & Engineering* Vol. 556, 2012, pp. 891–905.
- [16] Sohrab Enayatia, Seyed Ali Asghar Akbari Mousavi, Seyed Mohammad Ebrahimi, Majid Belbasic and Mostafa Sultan Bayazidi," Effects of Temperature and Effective Strain on the Flow Behavior of Ti–6Al–4V", *Journal of the Franklin* Vol.348 ,2011, pp 2813–2822.
- [17] Hossein Mohammadi and Mostafa Ketabchi," Backward Extrusion of 7075 Al Alloy in the Semisolid State", *International Journal of Chemistry and Material Science*, Vol. 1, No. 7, July, 2013, pp 182-188.
- [18] M.R. Rokni, A. Zarei-Hanzaki and H.R. Abedi," Microstructure Evolution and Mechanical Properties of Back Extruded 7075 Aluminum Alloy at Elevated Temperatures", *Materials Science and Engineering* Vol. 532, 2012, pp 593– 600.
- [19] Piotr Thomas," The Computer Simulation and the Experimental Research on the Stress Forces of the Combined Extrusion of Different Sized Aluminum Stampings", Vol. 5, 2013, pp 15 - 17.
- [20] T. Balusamy, Satendra Kumar and T. S. N. Sankara Narayanan, "Effect of Surface Nanocrystallization on the Corrosion Behaviour of AISI 409 Stainless Steel " *Corrosion Science*, Vol. 52, 2010, PP 3826-3834.